J Mater Sci (2009) 44:4026–4030
DOI 10.1007/s10853-009-3558-9

Spectroscopic properties of Nd^{3+}, Yb^{3+}-doped and Nd^{3+}–Yb^{3+}-codoped high silica glass

Yanbo Qiao · Ning Da · Danping Chen · Wenbo Ma · Qinling Zhou · Jianrong Qiu

Received: 25 February 2009 / Accepted: 9 May 2009 / Published online: 29 May 2009

Abstract The Nd^{3+}, Yb^{3+}-doped and Nd^{3+}–Yb^{3+}-codoped high silica glasses (HSGs) were fabricated by sintering porous glasses impregnated with Nd^{3+} and Yb^{3+} ions solutions. The Judd–Ofelt theory was used to study the spectroscopic properties of Nd^{3+}-doped HSGs. Large parameter Ω_2 of Nd^{3+}-doped HSGs suggests a lower centrosymmetric coordination environment around the Nd^{3+} in HSG. The spontaneous emission probability and emission cross-section (σ_{em}) of Yb^{3+}-doped HSGs are obtained. A broad emission band from 950 to 1,100 nm was detected when the Nd^{3+}–Yb^{3+}-codoped HSG was excited by 808 nm LD. The energy transfer process from Nd^{3+} to Yb^{3+} in HSG was described in this paper.

Introduction

To date, rare earth doped oxide glasses have attracted more and more attentions because of their increasing applications in lasers and amplifiers. Among various oxide glasses, silica is an attractive host matrix for rare earth (RE) ions because of its excellent optical and mechanical properties, such as good chemical stability, high UV transparency, strong thermal resistance, low nonlinear index, high surface damage threshold to lasers and large tensile fracture strength. However, concentration quenching of RE in silica glass is a problem which limits its application as a host matrix. Various methods have been used to suppress the concentration quenching, e.g., plasma-torch chemical vapor deposition (CVD) [1], sol–gel method [2] and modified sol–gel method using zeolite X [3]. Recently, some groups distribute RE or transition metal (TM) ions uniformly in porous glass and further heat treatment at a high temperature to obtain fluorescence high silica glass (HSG) [4–8]. The concentration quenching of the luminescence ions decreases because of the physical isolation of the nanopores. Moreover, the heat treatment temperature of the glass is lower than the melting temperature of the SiO_2. The RE or TM ions move difficultly in the solid state glass, so the ions clustering is prohibited in HSG. Nd^{3+}-doped HSG microchip has been fabricated by this method and the good laser performance from the microchip laser operating at 1.064 μm has been successfully demonstrated [9].

In this paper, Nd^{3+}, Yb^{3+}-doped and Nd^{3+}–Yb^{3+}-codoped HSGs were fabricated by sintering nanoporous glass impregnating with corresponding ions at 1,150 °C. Spectroscopic properties of Nd^{3+}, Yb^{3+}-doped and Nd^{3+}–Yb^{3+}-codoped HSGs were studied. The fluorescence intensities of the RE doped HSGs enhance when the Al_2O_3 was codoped in the glass. The content of SiO_2 in HSG is over 96%. Comparing other glass host, this HSG with composition of nearly pure SiO_2 shows high toughness for thermal loading. The material herein is expected to find applications in laser systems, especially high power and high repetition lasers.

Y. Qiao · N. Da · D. Chen (✉) · Q. Zhou
Shanghai Institute of Optics and Fine Mechanics, Chinese Academy of Sciences, Shanghai 201800, China
e-mail: dpchen2008@yahoo.com.cn

Y. Qiao · W. Ma
Research and Development Institute of Ocean's King Lighting, Shenzhen Ocean's King Lighting Science and Technology Co., Ltd, Shenzhen 518000, China

J. Qiu
College of Materials Science and Chemical Engineering, Zhejiang University, Hangzhou 310027, China

Experimental

Porous glass was obtained by removing the borate phase from phase-separated alkali-borosilicate glass by washing and leaching with hot acid solutions. The raw chemicals Na_2CO_3, $CaCO_3$, $Al(OH)_3$, SiO_2, H_3BO_3 were used as starting materials to produce mother glass ready for the preparation porous glass. The mother glass has a chemical composition of $51.7SiO_2$–$33.3B_2O_3$–$7.7Na_2O$–$4.0CaO$–$3.3Al_2O_3$ (wt%). The method is similar with the fabrication of Vycor glass developed by Corning Inc. The analytical composition of the porous glass was $97.0\%SiO_2$–$2.1\%B_2O_3$–$0.8\%Al_2O_3$–$0.1\%(Na_2O + CaO)$. The porous glass is a transparent material whose pore sizes are less than 4 nm, with pores nominally occupying about 30–40% of the glass volume. The porous glass was immersed in solutions of $Nd(NO_3)_3$, $Yb(NO_3)_3$ or mixed solutions of $Nd(NO_3)_3$ and $Yb(NO_3)_3$ for 1 h and dried at room temperature. The porous glasses impregnated with rare earth ions were then sintered at 1,150 °C for 2 h to obtain the final samples. Previous reports have indicted that sintering rare earth doped nanoprous glasses into compact material is a necessary step for preparing strong emission glass [4]. The sintering process can effectively reduce the impurity quenching effect of residual OH^- groups and the strong scattering of excitation lights due to the microscopic pores. Three series of rare earth doped HSGs were fabricated: Nd^{3+}-doped HSGs, Yb^{3+}-doped HSGs and Nd^{3+}–Yb^{3+}-codoped HSGs. It has been proved that codoping Al_2O_3 in silicate glass was good for the emission of rare earth [1]. We also fabricated some Nd^{3+}–Al^{3+}-doped, Yb^{3+}–Al^{3+}-doped and Nd^{3+}–Yb^{3+}–Al^{3+}-codoped HSGs. All of the samples look compact and transparent. The glass samples were cut and polished to $10 \times 10 \times 1.5$ mm^3.

Sample density was measured using the buoyancy method based on Archimedes principle using distilled water as the immersion liquid. The refractive index was measured with an Abbe refractometer. The density was 1.98 g/cm^3 and the refraction index 1.462. The absorption spectra were recorded with a Jasco V-570 UV/VIS/NIR spectrophotometer. The infrared luminescent spectra were obtained with ZOLIX SBP300 spectrophotometer excited by laser diode (LD) at 808 nm for Nd^{3+} and 980 nm for Yb^{3+}. The fluorescence lifetime was recorded with a modulated LD with a maximum power of 2 W. The frequency was modulated at 100 Hz and the signal, detected by an InGaAs photodetector in TRIAX550, was recorded using a storage digital oscilloscope (Tektronix TDS3052). All measurements were made at room temperature.

Results and discussions

Nd^{3+}-doped HSGs

Table 1 lists the obtained HSGs with different concentration of Nd^{3+} ions. The Judd–Ofelt [10, 11] intensity parameters $\Omega_{2,4,6}$ were obtained from the absorption spectra and listed in Table 1. Parameter Ω_2 reflects the intensity of the hypersensitive transition, whereas parameters Ω_4 and Ω_6 give an indication for the overall intensity of the spectral transition. Among the three intensity parameters, Ω_2 is most sensitive to the local structure and glass composition, which reflects the amount of covalent bonding and the asymmetry of the local environment near the rare earth site. We notice that the parameter Ω_2 in Nd^{3+}-doped HSGs are higher than in most silicate, fluoride, phosphate, borate, and aluminate glasses [12–16]. Large parameter Ω_2 suggests a lower centrosymmetric coordination environment around the Nd^{3+} in HSG.

Figure 1 shows the fluorescence spectra of Nd^{3+}-doped HSGs N1–N4. Sample N2 has the highest emission intensity when the Nd^{3+} ions concentration is 0.72×10^{20} ion/cm^3. The inset depicts the fluorescence intensity contrast of sample N1 and N5. An obvious increase in fluorescence intensity is observed after aluminum is codoped into Nd^{3+}-doped HSG. The fluorescence intensity of the sample N5 is about 3 times that of the sample N1. Table 2 lists the values of the peak wavelength of emission bands λ_e, the stimulated emission cross-sections of the transition $^4F_{3/2} \rightarrow {}^4I_{11/2}$ at 1,060 nm $\sigma_{1.06}$, τ_c, τ_m, and quantum efficiency η of HSG samples N1–N5. τ_m is fluorescence lifetime measured by fluorescence decay curve. τ_c is fluorescence lifetime calculated from the emission spectra. Detailed calculation of the values in Table 2 has been reported in a previous paper [7]. As shown in Table 2,

Table 1 Intensity parameters $\Omega_{2,4,6}$ of Nd^{3+}-codoped HSGs with different composition

Nd^{3+}-doped samples	Nd^{3+} (10^{20} ion/cm^3)	Al^{3+} (10^{20} ion/cm^3)	$\Omega_{2,4,6}$ (10^{-20} cm^2)		
			Ω_2	Ω_4	Ω_6
N1	0.36	0	5.07	3.98	2.24
N2	0.72	0	5.27	3.40	2.66
N3	1.08	0	5.41	3.20	4.27
N4	1.80	0	5.64	3.22	4.48
N5	0.36	1.80	7.16	3.20	2.97

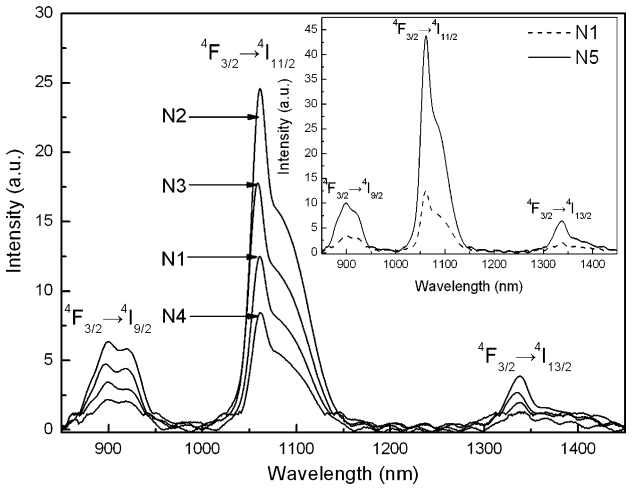

Fig. 1 Fluorescence spectra of Nd^{3+}-doped HSGs N1–N4. The inset depicts the fluorescence intensity contrast of N1 and N5

Table 2 Peak wavelength of emission bands (λ_e), stimulated emission cross-sections of the transition $^4F_{3/2} \rightarrow {}^4I_{11/2}$ ($\sigma_{1.06}$), measured fluorescence lifetime (τ_m) and calculated fluorescence lifetime (τ_c) of HSG samples N1–N5

Sample	λ_e (nm)	$\sigma_{1.06}$ (pm^2)	τ_m (μs)	τ_c (μs)	η (%)
N1	1,061	2.20	355	748	47.4
N2	1,061	2.23	340	727	46.8
N3	1,060	2.54	328	615	53.1
N4	1,060	2.49	320	621	51.5
N5	1,061	2.96	285	562	50.7

sample N5 has a larger stimulated emission cross-section than sample N1, indicating that adding aluminum into Nd^{3+}-doped HSG helps to increase its stimulated emission cross-section. Large stimulated emission cross-section is beneficial to a low threshold and a high gain in laser operations for a laser glass. The results show that codoped aluminum is available to accommodate the Nd^{3+} ions in a more energetically favorable environment [7, 17, 18].

Yb^{3+}-doped HSGs

Figure 2 shows the absorption spectra of Yb^{3+}-doped HSGs. Adding aluminum ions increases the absorption intensities of Yb^{3+}-doped HSG as shown in Fig. 2. The peak absorption cross-section σ_p and integrated absorption cross-section Σ_{abs} of 1.08×10^{20} ions/cm^3 Yb^{3+}-doped (sample Y1) and 1.08×10^{20} ions/cm^3 Yb^{3+}-1.08×10^{20} ions/cm^3 Al^{3+}-codoped (sample Y2) HSGs are calculated from the absorption spectra and listed in Table 3.

The inset of Fig. 2 shows the fluorescence spectra of the Yb^{3+}-doped HSGs excited by 980 nm LD. The fluorescent intensity increases when aluminum ion is codoped into the Yb^{3+}-doped HSGs. The fluorescent intensity of sample Y2 at 1,015 nm is about two times of sample Y1. Emission cross-section and fluorescent lifetime are usually used to evaluate laser glasses. These properties can be calculated using intensity parameters based on the Judd–Ofelt theory. Since there is only the $^2F_{5/2} \rightarrow {}^2F_{7/2}$ transition for Yb^{3+}, it is impossible to directly calculate the Judd–Ofelt parameters. The spontaneous emission probability (A_R) and the emission cross-section (σ_{em}) of Yb^{3+}-doped HSGs are calculated by Eqs. 1 and 2 [19] and listed in Table 3.

$$A_R = \frac{8\pi cn^2(2J'+1)}{\lambda_p^4(2J+1)N}\int K(\lambda)\mathrm{d}\lambda \quad (1)$$

$$\sigma_{em}(\lambda) = \frac{\lambda^4 A_R}{8\pi n^2 c\Delta\lambda_{eff}} \quad (2)$$

where c represents the velocity of light, n the refractive index, λ_p is the absorption peak wavelength, N is the concentration of Yb^{3+} ions, $K(\lambda)$ is the absorption coefficient, J' and J are the total momentum for the upper and lower levels and $\Delta\lambda_{eff}$ is the fluorescence effective linewidth. The measured fluorescent lifetime (τ_f) of samples Y1 and Y2 are also listed in Table 3. The emission cross-section increased from 0.65 pm^2 for sample Y1 to 0.82 pm^2 for sample Y2. $\sigma_{em}\tau_f$ is also an important parameter to evaluate laser properties of laser materials. $\sigma_{em}\tau_f$ of Yb^{3+}–Al^{3+}-codoped HSG is larger than Yb^{3+}-doped HSG. Our results indicate that Yb^{3+}–Al^{3+}-codoped HSG has better spectroscopic properties for a laser material.

Nd^{3+}–Yb^{3+}-codoped HSGs

The absorption spectrum of 0.72×10^{20} ions/cm^3 Nd^{3+}–0.36×10^{20} ions/cm^3 Yb^{3+}-codoped HSGs is shown in Fig. 3. The transition $^2F_{7/2} \rightarrow {}^2F_{5/2}$ peaking at 975 nm is attributed to the Yb^{3+} and the others are related to Nd^{3+} transitions. Figure 4 shows the fluorescence spectra of 0.36×10^{20} ions/cm^3 Nd^{3+}-doped and 0.36×10^{20} ions/cm^3 Nd^{3+}–0.36×10^{20} ions/cm^3 Yb^{3+}-codoped HSG excited by 808 nm LD. A broad emission band from 950 to 1,100 nm was detected when the Nd^{3+}–Yb^{3+}-codoped HSG was excited by 808 nm LD. The main peaks locate at about 970, 1,020, and 1,058 nm due to the $^2F_{5/2} \rightarrow {}^2F_{7/2}$ transition of Yb^{3+} and $^4F_{3/2} \rightarrow {}^4I_{11/2}$ transition of Nd^{3+}. The fluorescence intensity of Nd^{3+} excited by 808 nm decreases when the Yb^{3+} ions are codoped into the HSG. The inset of Fig. 4 compares the fluorescence intensities between Nd^{3+}–Yb^{3+}-codoped HSG and Nd^{3+}–Yb^{3+}–Al^{3+}-codoped HSG. Both the fluorescence intensities of Nd^{3+} and Yb^{3+} ions increase after the aluminum ions are codoped into the glass.

For Yb^{3+} ion, there is no absorption band near 808 nm. The infrared emission from single Yb^{3+}-doped glasses is

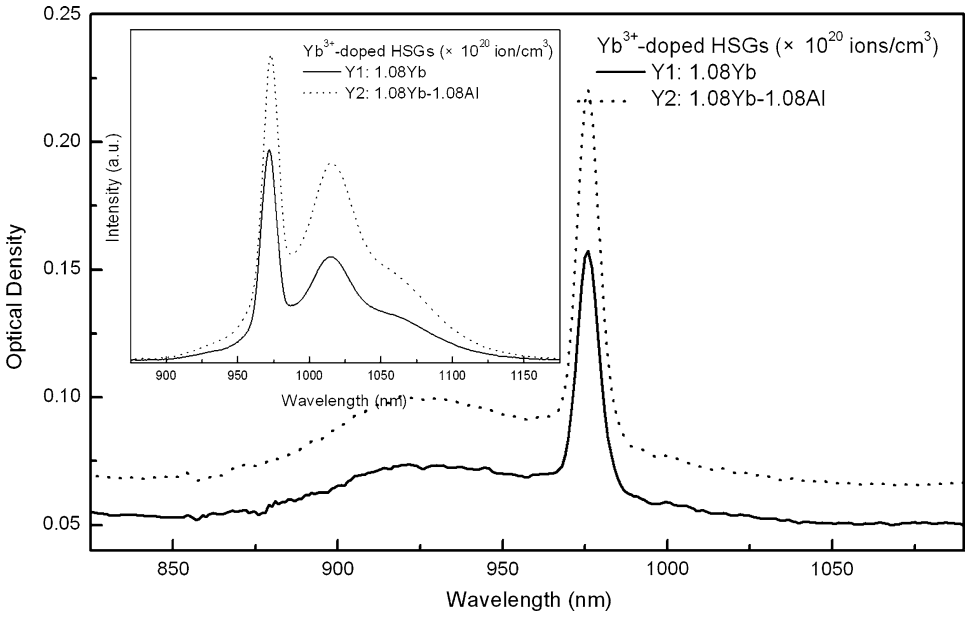

Fig. 2 Absorption spectra of Yb^{3+}-doped HSGs. The inset shows the fluorescence spectra of the Yb^{3+}-doped HSGs excited by 980 nm LD

Table 3 Spectroscopic properties of Yb^{3+}-doped HSGs

Yb^{3+}-doped samples	σ_p (pm^2)	$\sum_{abs}$ (10^4 pm^3)	σ_{em} (pm^2)	A_R (s^{-1})	τ_f (μs)	$\sigma_{em}\tau_f$ (pm^2 ms)
Y1	1.06	3.60	0.65	485.2	823	0.53
Y2	1.47	5.27	0.82	705.0	745	0.61

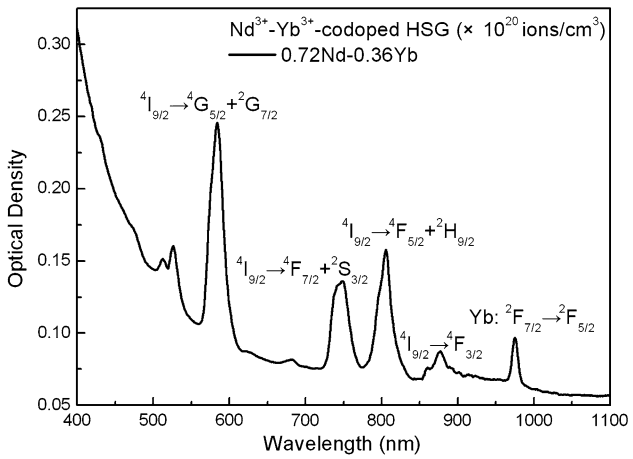

Fig. 3 Absorption spectrum of 0.72 × 10^{20} ions/cm^3 Nd^{3+}–0.36 × 10^{20} ions/cm^3 Yb^{3+}-codoped HSGs

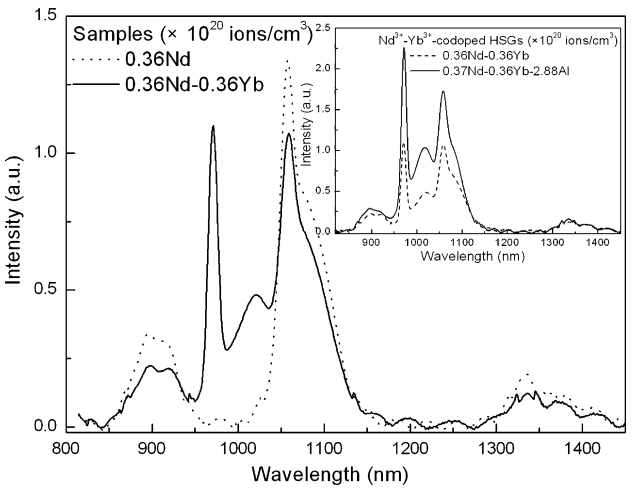

Fig. 4 Fluorescence spectra of Nd^{3+}-doped and Nd^{3+}–Yb^{3+}-codoped HSGs excited by 808 nm LD. The inset compares the fluorescence intensities between Nd^{3+}–Yb^{3+}-codoped HSG and Nd^{3+}–Yb^{3+}–Al^{3+}-codoped HSG

very weak when excited by 808 nm LD. The characteristic infrared emission of Yb^{3+} with peaks at 970 and 1,020 nm was detected when the Nd^{3+}–Yb^{3+}-codoped HSG was excited by 808 nm LD as shown in Fig. 4. It is indicated that there is energy transfer process from Nd^{3+} to Yb^{3+}. We note that the fluorescence intensity of Nd^{3+} at 1,060 nm becomes lower in the Nd^{3+}–Yb^{3+}-codoped HSG. Figure 5 shows the overlap of the emission spectrum of Nd^{3+} (the $^4F_{3/2} \rightarrow {}^4I_{9/2}$ transition) and the absorption spectrum of Yb^{3+} (the $^2F_{7/2} \rightarrow {}^2F_{5/2}$ transition). The Nd^{3+} and Yb^{3+} energy levels diagrams are represented in Fig. 6. The energy transfer process of from Nd^{3+} to Yb^{3+} was described by the scheme. When the Nd^{3+}–Yb^{3+}-codoped was excited by the 808 nm LD, the Nd^{3+} ions in the ground state absorb a photon to $^2H_{9/2}$ level and relax to $^4F_{3/2}$ level via a non-emission relaxation process, then the energy transfers

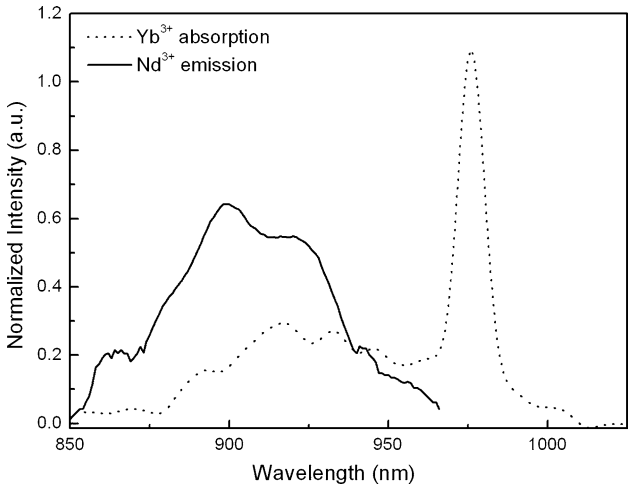

Fig. 5 Overlap of the emission spectrum of Nd^{3+} (the $^4F_{3/2} \rightarrow {}^4I_{9/2}$ transition) and the absorption spectrum of Yb^{3+} (the $^2F_{7/2} \rightarrow {}^2F_{5/2}$ transition)

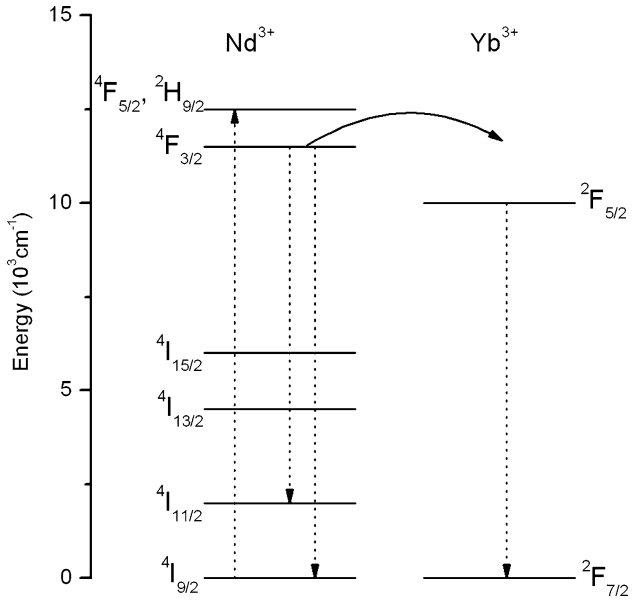

Fig. 6 Nd^{3+} and Yb^{3+} energy levels diagram. The energy transfer process of $Nd^{3+} \rightarrow Yb^{3+}$ is described

from the $^4F_{3/2}$ of Nd^{3+} to the $^2F_{5/2}$ of Yb^{3+}. Finally, the emission at 1,020 nm from Nd^{3+}–Yb^{3+}-codoped HSG occurs due to the transition of $^2F_{5/2} \rightarrow {}^2F_{7/2}$.

Conclusions

The Nd^{3+}, Yb^{3+}-doped and Nd^{3+}–Yb^{3+}-codoped high silica glasses were fabricated by sintering porous glasses impregnated with Nd^{3+} and Yb^{3+} solutions. The Judd–Ofelt intensity parameters $\Omega_{2,4,6}$ of Nd^{3+}-doped HSGs were obtained from the absorption spectra. Large parameter Ω_2 suggests a lower centrosymmetric coordination environment around the Nd^{3+} in HSG. The stimulated emission cross-sections of the transition $^4F_{3/2} \rightarrow {}^4I_{11/2}$ ($\sigma_{1.06}$) were obtained to evaluate the laser properties of Nd^{3+}-doped HSGs. The spontaneous emission probability and emission cross-section (σ_{em}) of Yb^{3+}-doped HSGs are calculated. $\sigma_{em}\tau_f$ of Yb^{3+}-Al^{3+}-codoped HSG is larger than Yb^{3+}-doped HSG, indicating that Yb^{3+}–Al^{3+}-codoped HSG has better spectroscopic properties for a laser material. The spectroscopic properties of Nd^{3+}–Yb^{3+}-codoped HSGs were studied. The Nd^{3+}–Yb^{3+}-codoped HSGs has a broad emission from 950 to 1,100 nm because of the $^2F_{5/2} \rightarrow {}^2F_{7/2}$ transition of Yb^{3+} and $^4F_{3/2} \rightarrow {}^4I_{11/2}$ transition of Nd^{3+} when excited by 808 nm LD. The energy transfer process from Nd^{3+} to Yb^{3+} was described in this study.

Acknowledgement This work was financially supported by National Natural Science Foundation of China (Grant No. 60707019 and No. 60778039).

References

1. Arai K, Namikawa H, Kumata K, Honda T, Ishii Y, Handa T (1986) J Appl Phys 59:3430
2. Thomas IM, Payne SA, Wilke GD (1992) J Non-Cryst Solids 151:183
3. Fujimoto Y, Nakatsuka M (1997) J Non-Cryst Solids 215:182
4. Chen D, Miyoshi H, Akai T, Yazawa T (2005) Appl Phys Lett 86:231908
5. Qiao Y, Chen D, Ren J, Wu B, Qiu J, Akai T (2008) J Appl Phys 103:023108
6. Sharonov MY, Myint T, Bykov AB, Petricevic V, Alfano RR (2007) J Opt Soc Am B 24:2868
7. Qiao Y, Da N, Chen D, Zhou Q, Qiu J, Akai T (2006) Appl Phys B 87:717
8. Qiao Y, Wen L, Wu B, Ren J, Chen D, Qiu J (2007) Mater Chem Phys 107:488
9. Xia J, Chen D, Qiu J, Zhu C((2005) Opt Lett 30:47
10. Judd BR (1962) Phys Rev 127:750
11. Ofelt GS (1962) J Chem Phys 37:511
12. Krupke WF (1974) IEEE J Quantum Electron 10:450
13. Balda R, Fernández J, Mendioroz A, Adam JL, Boulard B (1994) J Phys Condens Matter 6:913
14. Nageno Y, Takabe H, Morinaga K (1993) J Am Ceram Soc 76:3081
15. Gatterer K, Pucker G, Fritzer HP, Arafa S (1994) J Non-Cryst Solids 176:237
16. Uhlmann EV, Weinberg MC, Kreidl NJ, Burgner LL, Zanoni R, Church KH (1994) J Non-Cryst Solids 178:15
17. Monteil A, Chaussedent S, Alombert-Goget G, Gaumer N, Obriot J, Ribeiro SJL, Messaddeq Y, Chiasera A, Ferrai M (2004) J Non-Cryst Solids 348:44
18. Alombert-Goget G, Gaumer N, Obriot J, Rammal A, Chaussedent S, Monteil A, Portales H, Chiasera A, Ferrari M (2005) J Non-Cryst Solids 351:1754
19. Zou X, Toratani H (1995) Phys Rev B 52:15889